

Fragmentation Phase Transition in Atomic Clusters II

— Symmetry of Fission of Metal Clusters —

M.E. Madjet, P.A. Hervieux [◊], D.H.E. Gross, and O. Schapiro

Hahn-Meitner-Institut Berlin, Bereich Theoretische Physik, Glienickerstr.100
14109 Berlin, Germany

and

Freie Universität Berlin

[◊] Institut de Physique, Lab LPMC, 1 Bd Arago, F57078 Metz Cedex 3,
France

May 10, 2021

Abstract

We present a statistical fragmentation study of doubly charged alkali (Li, Na, K) and antimony clusters. The evaporation of one charged trimer is the most dominant decay channel (asymmetric fission) at low excitation energies. For small sodium clusters this was quite early found in molecular dynamical calculations by Landman et al. [1]. For doubly charged lithium clusters, we predict Li_9^+ to be the preferential dissociation channel. As already seen experimentally a more symmetric fission is found for doubly charged antimony clusters. This different behavior compared to the alkali metal clusters is in our model essentially due to a larger fissility of antimony. This is checked by repeating the calculations for Na_{52}^{++} with a bulk fissility parameter set artificially equal to the value of Sb.

1 Introduction

Doubly ionized clusters are not stable if the Coulomb repulsion energy between the two positive holes exceeds the binding energy. The first experimental evidence for Coulomb explosion of doubly charged clusters is due to

Sattler et al. in 1981 [2]. Cluster stability of multiply charged simple metal clusters is usually studied after either increasing the internal energy or the charge state by laser excitation [3] or by collision with charged particles [4]. The size of the surviving clusters depends on their charge state. The higher the charge the larger the cluster must be to compensate the electrostatic pressure by adhesive forces. It is worth noting that the critical sizes measured in these two experiments are different. This might be due to different temperatures at which the clusters are produced by the two methods. Also the deexcitation mechanism is different for different clusters. For singly charged alkali metal clusters, experiments done by Bréchignac et al. have shown that the excess of internal energy is dissipated by successive evaporation of either neutral monomers or dimers [5, 6, 7]. In contrast, singly charged antimony clusters relax their excess of energy by evaporation of tetramers [8].

Small doubly charged alkali clusters, due to the large surface tension of the bulk material and due to the mobility of the electrons, fission asymmetrically. Because of strong shell effects the emission of a charged trimer is the most preferential dissociation channel. This asymmetric fission of doubly charged alkali clusters is in sharp contrast to fission of nuclei where the charge degree of freedom is strongly linked to that of the mass by the symmetry force. Therefore nuclear fission is much more symmetric. The experiments determined the smallest mass a stable cluster can have with given charge, the critical size of stability (clusters with mass smaller than 36 for $Z = 2$ become unstable) [5, 9, 10]. It is, however, not true that extreme asymmetric fission is a genuine feature of fission of doubly charged metal clusters. In a recent experiment Bréchignac et al. [11] found that larger doubly charged antimony clusters fission the more symmetrically the larger the clusters are. Why does fission occur symmetrically in some cases and asymmetrically in others ?.

The traditional method to describe the fission of atomic clusters is by molecular dynamics (*MD*). Here one follows the classical Newtonian equation of motion of the interacting many-atom system. In contrast to Lenard-Jones systems for which the interatomic potential is known, metal clusters, due to the delocalization of the valence electrons, do not have well defined interatomic potentials. Therefore, it is difficult to carry out *MD* calculations for metal clusters. One has to combine this with an explicit treatment of the electronic degrees of freedom of the whole cluster like e.g. a Kohn-Sham calculation [1] which is restricted to smaller systems. By using a n-body potential (which reproduces the bulk properties) to model neutral metal clusters,

López et al.[12] have investigated the fragmentation process at low excitation energies and for clusters containing no more than 14 atoms by *MD*. Garcias et al. in a series of papers [13] used density-functional theory in two jellium spheres to evaluate the fusion barriers for different doubly charged alkali metal clusters.

Encouraged by the experience that the dynamics of interacting many-body systems is often ergodic and is thus mainly controlled by the structure of the accessible N-body phase space, we try Microcanonical Thermodynamics. A detailed introduction into Microcanonical Thermodynamics is given in [14].

In this paper we investigate the coulombic fission of doubly charged metal clusters of less than 60 atoms as a function of the excitation energy. We study in particular how the excitation energy will be partitioned among the internal, translational, rotational and charged degrees of freedom. In using the Microcanonical Metropolis Monte Carlo method (*MMMC*), described in details in [15, 14], see also the first paper of this series [16], we present the fragmentation of doubly charged clusters of the elements Li, K, Na and Sb. In the next paper of this series [17] we will study the implication of the accessible phase space on the fragmentation of multiply ($Z \geq 2$) charged alkali clusters. A fourth paper [18] will discuss the relation of the fragmentation phase-transition to the liquid-gas transition of the bulk.

2 The effect of the bulk entropy

The internal entropy of larger clusters is close to the entropy of the bulk material at the same specific excitation energy. It is just one of the main advantages of *MMMC* that it does not follow the individual motion of each atom but allows incorporating known properties of the bulk material. This is the more important as the internal behavior of the cluster becomes quite complicated near structural transitions of the bulk. E.g. near melting high anharmonicities evolve[19] which are extremely difficult to describe microscopically.

Knowledge of the specific heat at constant pressure of metals (commonly at atmospheric pressure) is fundamental for the description of their thermodynamic behavior. Using this quantity and the latent specific heat, one can compute other thermodynamic properties like the entropy or the internal energy as a functions of temperature [19].

Experiments involving alkali metal clusters are often carried out at finite temperature, generally above the bulk melting temperature (for Na $T_m \approx 400$ K). The clusters behave more like hot liquid droplets and the harmonic (Debye) approximation is no longer valid to describe correctly the internal behavior of the clusters. For the particular case of antimony clusters, however, which have a much higher bulk-melting temperature ($T_m = 904$ K), one could expect the temperature of the clusters produced to be lower than the melting temperature but still the effects of anharmonicities remain important and have to be taken into account. The experimental bulk specific heat is taken from refs.[20, 21]. For antimony, as far as we know, there are no data available for the very low temperatures below $T = 298$ K. Here anharmonicities become unimportant and the specific heat can be computed within the Debye model, i.e. assuming the internal degrees of freedom to be harmonic oscillators. The dependence of the specific entropy s on the specific excitation energy ε for the different elements studied are shown in Fig.1. The Debye temperature gives the temperature above which all vibrational modes are excited. Below this temperature, the modes begin to be frozen out. For alkali metals the element with the smallest Debye temperature has the largest entropy over the entire range of excitation energies (the Debye temperatures θ_D are reported in Tab.I). This is a consequence of the dependence of the specific heat at low temperature on the Debye temperature. One remarks also that the specific entropy of antimony is very close to that of sodium. In fact, these two elements have similar Debye temperatures.

As pointed out by N. Ju and A. Bulgac [22], the finite temperature properties of simple metal clusters, in particular phase transitions, are dominated by the ionic degrees of freedom as a consequence of the very small contribution to the entropy coming from the electrons. Therefore, in the present model we ignored the influence of the valence electrons on the entropy (e.g. through shell effects as discussed in ref.[23]).

Our physical scenario of statistical cluster fission is as follows: We assume the dynamics of a cluster to be sufficiently chaotic after it was excited by a laser or by a passing heavy ion. If this hypothesis is correct the cluster will fission highly ergodically. That means many replicas of the reaction with the same macroscopic initial conditions, impact parameter, excitation energy etc., explore the details of the topological structure of the N-body phase space which is accessible under the constraints of the global conservation of energy, angular momentum, mass, and charge. We further *assume* that the

stochastic coupling of the fragment motion has a short range very similar to the strong and short range friction which acts between the moving fragments in nuclear fragmentation [24]. This hypothesis is still to be proven. However, it allows to simplify highly the general complicated expansion dynamics of the decay. By this assumption it is possible to subsume all details under two fit parameters, the freeze-out volume outside of which the stochastic coupling of the fragments ceases and the maximum internal excitation energy ε_{max} of the fragments.

Inside the freeze-out volume with a radius

$$R_{sys} = r_f * N^{1/3}$$

the cluster and its fragments are strongly stochastically coupled and explore the accessible phase space. Outside of it the various fragments disassemble independently (besides an eventual Coulomb interaction between the fragments).

The second parameter of our fragmentation model as defined in ref.[15] is the maximum specific internal energy per atom which is allowed for the fragments (ε_{max} see Tab.I). In analogy to our previous study on the fragmentation of hot sodium clusters, ε_{max} is estimated by the assumption that inside the freeze-out configuration the excited clusters should live longer than the lifetime of the freeze-out configuration itself. Fragments excited to higher energies decay inside the freeze-out configurations and these excitations are counted as excitations of the daughter-fragments. Moreover, the system is assumed to be in equilibrium within the freeze-out volume. Therefore, the evaporation times of the fragments (calculated within the Weisskopf model) corresponding to $\varepsilon \leq \varepsilon_{max}$ must be also larger than the characteristic time associated to the interaction between the atoms (period of vibration) inside each fragment.

It was mentioned by N. Ju and A. Bulgac [22] the melting and boiling temperatures of sodium clusters do not seem to be strongly dependent on the particle number. This behavior is at variance to that of tin clusters [25] and justifies our assumption to take ε_{max} (at least for Na) to be independent of the particle number.

3 Alkali Metal Clusters

The ground state binding energies are computed within the metallic liquid drop model. First we need the barriers for charged particle decay. These must be calculated from the electrostatic energy between two charged metallic spheres. This is done by iterating the induced image charges. According to a recent paper of Seidel and Perdew [26], who have solved the classical image potential paradox, we have modified the formula (13) given in ref.[15]. The parameters which enter in this formula are given in Tab.I. In order to take into account the electronic shell effects which are important for small clusters, we have used, if available, the experimental binding energies instead of those from the metallic liquid drop model. For singly charged clusters we have used the binding energies given in refs.[5, 6, 7] for Li, Na, and K, respectively. From the knowledge of the experimental ionization potentials [27, 28, 29, 30] it is possible to get the binding energies for neutral clusters up to the size 26, 21, and 26 for Li, Na, and K, respectively.

In our fragmentation model, since the properties of diatomic or the triatomic molecules are well known, we used for dimers and trimers the values of the vibrational frequencies and the calculated principal moments of inertia given in Tab.I. We have improved our model by taking polarization effects into account [17]. As discussed in details in ref. [17], we do not allow the fragments to be closer than a certain distance which is fixed at 1.0 Å for all the elements studied.

Initial clusters having 30, 42 and 52 atoms decay quite differently because of shell effects in the daughters. For the sizes 30 and 42, the daughters from the fission process may have both magic number of electrons (i.e. $X_{30}^{++} \rightarrow X_{21}^+ + X_9^+$ and $X_{42}^{++} \rightarrow X_{21}^+ + X_{21}^+$). Fission of Na_{52}^{++} which does not fulfill the last property was taken as a third example. We calculated the distribution of the three largest average masses as a function of the specific excitation energy for the different initial cluster sizes. As neutral monomers are not considered as fragments they are not included in the mass distribution presented here. The fragments can be either charged or neutral.

In Fig.2 we present the results for a fissioning cluster of size 30. Lithium clusters, at $\varepsilon \lesssim 0.25$ eV/atom decay only into Li_{21}^+ and Li_9^+ . One notes that this fission channel is the only one. Above $\varepsilon \approx 0.3$ eV/atom one sees the appearance of a neutral fragment and at $\varepsilon \gtrsim 0.4$ eV/atom the system decays into more than three fragments. Within the statistical model the thermody-

namic temperature is in the energy range $0.05 \text{ eV/atom} \leq \varepsilon \leq < 0.4 \text{ eV/atom}$ a linear function of ε varying from 335 K to 1200 K. In contrast to Na and K for which the singly charged trimer is the most stable cluster, Li_9^+ has the highest stability. We have checked that at low excitation energy ($\varepsilon < 0.25 \text{ eV/atom}$) the fission pattern is not sensitive to the internal entropy of the fragments. In this case the sampling of the internal excitations was performed by using a harmonic level density (classical Einstein model) [15] with a single vibrational frequency. Our finding of a dominating decay into a Li_9^+ is in contradiction with the experiment [31]. In fact, experimentally the trimer is still the preferential fission channel, the production of Li_9^+ exists but with a much lower probability. As already mentioned above, one cannot explain the experimental results in using only energetic considerations and it seems that also our statistical approach is not able to reproduce the experimental trends for the fission of Li_n^{++} . One must recall that the statistical theory ignores any information about the dynamics of fragmentation. Consequently, one may think that there is a dynamical mechanism which plays a role in the fission process. Other possible reasons for the failure of our statistical multifragmentation model here may be the neglect of nonsphericities of the Li trimers which taken into account could well lower the barriers for the trimer decay. At this moment we are unable to decide this.

The calculations for Na_{30}^{2+} are presented in fig.2b. At very low energy $\varepsilon < 0.07 \text{ eV/atom}$ the system evaporates one neutral monomer. Above this energy the system decays into one large and one small singly charged fragment. There is a competition between the emission of Na_3^+ and Na_9^+ the latter fragment having the largest probability. One notes that besides these two channels we have also the presence of other fragments but with much lower probability. At an energy above 0.20 eV/atom, the system prefers to fragment into three or more fragments of intermediate sizes. It is worth noting that the energy at which the multifragmentation takes place is higher for Li than for Na and this is a direct consequence of a larger cut-off of the bulk excitation energy ε_{max} of Li (see Tab.I).

K_{30}^{2+} decays, at very low energy, $\varepsilon < 0.07 \text{ eV/atom}$, like Na_{30}^{2+} by evaporating one neutral monomer, see figure 2c. However, above this energy the ejection of a singly charged trimer is the preferred fission channel. When the excitation energy increases the number of channels increases but trimer ejection remains the dominant mode of decay. For higher energies ($\varepsilon > 0.2 \text{ eV/atom}$) the system follows the same scenario as described above for Na.

Due to similar values of ε_{max} for Na and K, the multifragmentation mode appears at about the same energy.

Let us now discuss the clusters of sizes 42, see fig.4 for Li, below 0.1 eV/atom we have emission of Li_9^+ . Above this energy, the fragment Li_9^+ remains the most probable product of fission but one sees the appearance of symmetric fission through the production of two fragments of equal sizes. There is also the presence of other fragments but with much less probability. When the energy is increasing the fission process becomes more and more symmetric. This is clearly illustrated in Fig.4 where we have plotted the relative probability as a function of the mass of the fragments at two excitation energies.

For Na_{42}^{++} , below $\varepsilon \approx 0.1$ eV/atom we have evaporation of one neutral monomer. For $0.1 \text{ eV/atom} < \varepsilon < 0.3 \text{ eV/atom}$ there is a competition between Na_3^+ and Na_9^+ and no presence of Na_{21}^+ . From 0.1 eV/atom to 0.2 eV/atom Na_3^+ is dominant. From 0.2 to 0.3 eV/atom Na_9^+ is dominant. Note, that compared to Na_{30}^{++} the fragmentation region shifts upwards in energy and becomes more sharp. The thermodynamic temperature shows at $\varepsilon \sim 0.3$ eV/atom a backbending signalizing a phase transition of first order. Evidently this cluster is large enough to show the fragmentation phase transition.

For K_{42}^{++} , the distribution is rather similar to that of K_{30}^{++} . Here also the fragmentation is shifted to higher energy. Again a first order transition towards fragmentation is clearly seen as a backbending in $T(\varepsilon)$.

The size 52 is interesting to study since the fission into two fragments having both closed shells is no longer possible. As it can be seen in Fig.5a, for Li, over the whole range of energy up to the transition energy ($\varepsilon \approx 0.4$ eV/atom) Li_9^+ is the preferential dissociation channel. In contrast with Li_{42}^{++} , the production of Li_{21}^+ is non-existent. For Na_{52}^{++} and K_{52}^{++} , the results are shown in Figs.5b and c. In all clusters of this size the first order transition towards fragmentation can clearly be seen. A comment may be necessary on the high thermodynamic temperatures the system can get in the range of excitation energies studied: They are finally *larger* than the boiling temperature of the bulk. Here one has to keep in mind that because of the assumed short range of the possible interfragment friction our calculations are at constant freeze-out *volume* not at constant pressure as in studies of boiling of the bulk, see further discussion of this point in the fourth paper of this series [18].

4 Antimony Clusters

It has been observed experimentally [11] that antimony clusters exhibit a completely different behavior with respect to alkali metal clusters. For sizes around 44, antimony prefers to fission into two singly charged clusters with similar sizes and this can not be explained in terms of electronic shell effects.

Due to the lack of experimental and theoretical data for this type of clusters, we were forced to make several assumptions. We considered antimony clusters to have metallic character and therefore the binding energies of the charged species will be computed within the metallic liquid drop model. Thus the later finding of a more symmetrical fission than Na-clusters (as found in the experiments) is within our phase space model *not* due to a different conductivity and charge distribution. Even with the extreme assumption of a metallic conductivity as in alkali clusters Sb^{++} -clusters fission more symmetrically. For neutral and singly charged dimers and trimers we have used the experimental binding energies given in ref.[32] and their moments of inertia were computed from the theoretical data of [33]. The surface energy a_s is calculated from the bulk value of the surface tension α ($a_s = 4\pi r_s^2 \alpha$), here r_s is the Wigner-Seitz radius.

The computed mass distributions are shown in Fig.6 for the mass 30, 42, and 52. At low energy, the system breaks into two singly charged fragments having comparable sizes. As the energy is increasing one observes the appearance of a third fragment namely a neutral dimer or a neutral quadrimer. Depending on the initial cluster size, above a certain energy the preferential third fragment is Sb_4 . This production of Sb_4 is artificial since we have taken the experimental binding energies for the dimers and trimers and used the liquid drop model to compute the binding energies of the other fragments. The caloric curve $T(\varepsilon)$ is much more smooth than for Na-clusters. This is so because this is far below the bulk-boiling of antimony which is at 1907 K.

Quantitative predictions by our statistical model of the symmetrical character of the fission process for clusters having at least 52 atoms compare favorably with the experimental results [11].

The ground state fissility parameter f is defined as the ratio of the Coulomb energy E_C to the surface energy E_S and within the metallic liquid drop model can be expressed as :

$$f = \frac{E_C}{2E_S} = \chi \frac{Z^2}{N} \quad (1)$$

$$\chi = \frac{e^2}{4r_s a_s} \quad (2)$$

where Z and N are the charge and the mass of the initial cluster. Let us take the example of a cluster of size 52 and charge 2, $f = 0.12, 0.13, 0.11$ and 0.62 for Li, Na, K and Sb respectively. One immediately notes that Sb has a fissility ≈ 5 times larger than the other alkali metal elements.

Another useful quantity is the asymmetry parameter η which is defined as the ratio between the size difference of the two singly charged fragments to the parent size. η is a function of the temperature and of the initial cluster size. If one wants to compare theoretical and experimental results, one needs to have an estimate of the temperature at which the experiment was carried out. It comes out from the model that for Sb_{52}^{++} , $\eta \approx 0.15$ at a thermodynamic temperature of about 300 K (far below the melting temperature $T_m = 904$ K !). This must be compared to the experimental result $0.27 \leq \eta \leq 0.34$ [11]. Unfortunately, in the ref.[11] the temperature was not given.

A possible explanation of this disagreement is given by the fact that we have used in our calculations the value of the bulk surface tension to compute the surface energy a_s^B . However, we know that a_s must be modified in order to take finite size effects into account and usually the corrected value of a_s is larger than the one of the bulk (e.g. for Na, $a_s^B = 0.80$ eV and $a_s = 1.02$ eV [5]). Consequently according to formula 2, the fissility decreases and the fission becomes less symmetrical. In using the same ratio (a_s/a_s^B) as for Na, we have performed again the calculations and we have found $\eta \approx 0.27$ which is in better agreement with the experimental values. Also non perfect metallic conductivity would lead to more symmetric fission.

Using the liquid drop model we observe that the fragmentation does not evolve with increasing cluster size from an asymmetric to a symmetric fission which is in disagreement with the experiment. A possible reason is : For low masses (here 30 and 42), one observes experimentally an asymmetric fission with a predominance for Sb_5^+ and Sb_7^+ as small fragments. This behavior seems analogous to the shell effects of alkali metal clusters. In contrast to our precedent study on alkali metals, and due to lack of experimental data no shell effects have been included in our present calculations.

To gain a basic understanding of the role played by the surface energy on the fission process, we have calculated the average three largest masses as a function of the excitation energy for Na_{52}^{++} in using a value of a_s which corresponds to the same fissility as for Sb_{52}^{++} (of course in the pure liquid drop approximation for the binding energies). The results of the computation are shown in Fig.7. One should mention that both Na and Sb have nearly identical entropies over the entire excitation energy range (see Fig.1). The distribution is surprisingly similar to that of Sb_{52}^{++} (see Fig.6c). One concludes that the symmetrical character of the fission seems to be mainly governed by the smaller surface tension and the smaller Wigner-Seitz radius of bulk antimony in the same combination of the two as is expressed by the fissility parameter χ . There is however, a remarkable difference to nuclear fission: In metal cluster fragmentation one can vary charge and mass independently of one another within some margins. Increasing the charge the fissility rises according to formula (1). Instead of shifting to more symmetric binary fission, Na_n^{Z+} decays into several (up to Z) charged fragments. Below the fragmentation transition one is heavy, often doubly charged, and the others are singly charged nine-mers or trimers. The heavy one has a low fissility again. This is not possible in nuclear fission as there the mass to charge ratio of the fragments can not vary so much.

Further, we hope that the experimentalists in the near future will be able to measure the binding energies of singly charged antimony clusters. From these values we could get a more realistic value of a_s . An indication of the temperature at which the experiments are carried out is necessary.

5 Conclusions

We have shown that the symmetry of fission of doubly charged metal clusters is ruled by the number of exit channels (phase space) which are energetically accessible (calculated within the framework of our statistical fragmentation model *MMMC*) and depends on:

- the initial cluster size,
- the initial excitation energy,
- the bulk surface tension and the bulk density (combined to the fissility parameter χ),

- and the electronic shell effects through the ground state binding energies of the fragments.

For Li the dominant decay channel is always Li_9^+ . This behavior is in contradiction to the experiment. This disagreement might be due to a dynamical mechanism or due to deformation effects which are not taken into account in our statistical model. For Li_{42}^{++} we find at high enough excitation energies a symmetric fission (with a probability of $\approx 30\%$) as a consequence of the closed electronic shell of Li_{21}^+ .

At low excitation energy, below the multifragmentation transition, for Na and K clusters, the fission is always asymmetric whatever is the initial size. For a given size, when the excitation energy increases, the number of dissociation channels increases as well. There is a competition between the different channels which are energetically favored by electronic shell effects.

This study demonstrates that the symmetry of the fission process which has been observed experimentally for doubly charged antimony clusters of intermediate size can be interpreted in terms of the larger bulk fissility parameter χ .

Finally, our calculations have shown that it is possible to classify the effects shaping the fission pattern into two types according to their origin : electronic shell effects through the ground state binding energies and the bulk fissility.

6 Acknowledgment

The Sonderforschungsbereich SFB 337 of the DFG supported this work by granting a post-doc position (M.Madjet). The Fachbereich Physik of the Freie Universität Berlin made this work possible by giving access to their computer system.

Figure 1: Specific entropy of bulk sodium, potassium, lithium and antimony at atmospheric pressure as a function of the specific internal energy.

Figure 2: Average masses of the three largest fragments as a function of the specific internal energy for the clusters: (a) Li_{30}^{2+} , (b) Na_{30}^{2+} and (c) K_{30}^{2+} . The dashed curve shows the caloric curve $T(E)$ in Kelvin. In this subsection quadrupoles and heavier fragments are assumed to be conducting spheres.

Figure 3: Same as Fig.2 but for: (a) Li_{42}^{2+} , (b) Na_{42}^{2+} and (c) K_{42}^{2+} .

Figure 4: Mass distribution of Li_{42}^{2+} at a specific excitation energy: (a) $\varepsilon = 0.12$ eV/atom and (b) $\varepsilon = 0.214$ eV/atom.

Figure 5: Same as Fig.2 but for: (a) Li_{52}^{2+} , (b) Na_{52}^{2+} and (c) K_{52}^{2+} .

Figure 6: Same as Fig.2 but for: (a) Sb_{30}^{2+} , (b) Sb_{42}^{2+} and (c) Sb_{52}^{2+} .

Figure 7: Average masses of the three largest fragments as a function of the specific internal energy for the cluster Na_{52}^{2+} with a modified surface energy $a_s = 0.218$ eV.

Table 1: Experimental and theoretical values of the different parameters used in our calculations. r_s is the Wigner Seitz radius [34] a_v is the volume cohesion energy and a_s its surface part [5, 34]. The work function for ionisation of the bulk W_∞ [34, 35], the ionization energy of the atom IP [34], the radius of the freeze-out configuration r_f , the principal moments of inertia for the dimer I_2 [36, 37] and for the trimer I_3 [38, 39, 40, 33], the Debye temperature θ_D [41, 20], the melting and boiling temperatures T_m and T_v [20, 34], the dimer and trimer frequencies ω_d [37] and ω_t [42], the maximum specific internal energy of the bulk ε_{max} , and the bulk fissility coefficient χ . For simplicity we used in all cases for ε_{max} the boiling energy at normal pressure. This corresponds to $\tau_{evap} = \tau_{\varepsilon_{max}} \approx 10^{-11}$ secs. In the case of Sb the excitation of the fragments never reached values of $\varepsilon = \varepsilon_{max}$

Element	Li	Na	K	Sb
$r_s(\text{\AA})$	1.719	2.070	2.571	1.130
$W_\infty(\text{eV})$	2.490	2.751	2.299	4.550
$IP(\text{eV})$	5.361	5.140	4.340	8.640
$a_s(\text{eV})$	1.301	1.020	0.980	0.397
$a_v(\text{eV})$	1.521	1.121	0.939	2.751
$\theta_D(\text{K})$	345.	150.	90.	140.
$\omega_d(\text{eV})$	$4.352E - 2$	$1.490E - 2$	$1.141E - 2$	$1.206E - 2$
$\omega_t(\text{eV})$	$2.973E - 2$	$1.048E - 2$	$7.755E - 3$	$1.206E - 2$
$\varepsilon_{max}(\text{eV/atom})$	0.460	0.350	0.330	0.750
$\tau(\varepsilon_{max})(\text{secs})$	$1.85E - 11$	$5.33E - 11$	$3.15E - 11$	$2.18E - 8$
$I_2/m_0(\text{\AA}^2)$	3.56	4.74	7.64	2.71
$I_{3x}/m_0(\text{\AA}^2)$	2.94	4.84	7.45	3.15
$I_{3y}/m_0(\text{\AA}^2)$	7.88	5.66	8.63	3.71
$I_{3z}/m_0(\text{\AA}^2)$	10.82	10.49	15.62	6.86
$T_m(\text{K})$	453.65	370.95	336.60	904.00
$T_v(\text{K})$	1600.00	1156.00	1033.00	1907.00
$r_f (\text{\AA})$	3.20	3.85	4.78	2.10
χ	1.60	1.69	1.42	7.96

References

- [1] R.N. Barnett, U. Landman, and G. Rajagopal. Patterns and barriers for fission of charged small metal clusters. *Phys. Rev. Lett.*, 67:3058, 1991.
- [2] K. Sattler, M. Mühlbach, O. Echt, P. Pfau, and E. Recknagel. *Phys. Rev. Lett.*, 47:160, 1981.
- [3] U. Näher, S. Frank, M. Malinowski, U. Zimmermann, and T.P. Martin. Fission of highly charged alkali metal clusters. *Z. Phys. D*, 31:191, 1994.
- [4] F. Chandezon, C. Guet, B.A. Huber, D. Jalabert, M. Maurel, E. Monnand, C. Ristori, and J.C. Rocco. *Phys. Rev. Lett.*, 74:3784, 1995.
- [5] C. Bréchignac, H. Busch, Ph. Cahuzac, and J. Leygnier. *J. Chem. Phys.*, 101:6992, 1994.
- [6] C. Bréchignac, Ph. Cahuzac, J. Leygnier, and J. Weiner. Dynamics of unimolecular dissociation of sodium cluster ions. *J. Chem. Phys.*, 90:1492, 1989.
- [7] C. Bréchignac, Ph. Cahuzac, F. Carlier, M. de Frutos, and J. Leygnier. *J. Chem. Phys.*, 93:7449, 1990.
- [8] D. Rayane, P. Melinon, B. Tribollet, B. Cabaud, A. Hoareau, and M. Broyer. *J. Chem. Phys.*, 91:3100, 1989.
- [9] C. Bréchignac, Ph. Cahuzac, F. Carlier, and M. de Frutos. Asymmetric fission of Na_n^{++} around the critical size of stability. *Phys. Rev. Lett.*, 64:2893, 1990.
- [10] C. Bréchignac, Ph. Cahuzac, F. Carlier, J. Leygnier, and A. Sarfati. *Phys. Rev. B*, 44:11386, 1991.
- [11] C. Bréchignac, Ph. Cahuzac, F. Carlier, J. Leygnier, and J.Ph. Roux. *J. Chem. Phys.*, 102:1, 1995.
- [12] M.J. López and J. Jellinek. Fragmentation of atomic clusters: A theoretical study. *Phys. Rev. A*, 50:1445, 1994.

- [13] R.J. Garcias, R.J. Lombard, M. Baranco, J.A. Alonso, and J.M. López. *Z. Phys. D*, 33:301, 1995, and references therein.
- [14] D.H.E. Gross. Microcanonical thermodynamics and statistical fragmentation of dissipative systems — the topological structure of the n-body phase space. *Physics Reports*, 1996 in preparation.
- [15] D.H.E. Gross and P.A. Hervieux. Statistical fragmentation of hot atomic metal clusters. *Z. Phys. D*, 35:27–42, 1995.
- [16] D.H.E. Gross, M.E. Madjet, and O. Schapiro. Fragmentation phase transition in atomic clusters I — microcanonical thermodynamics. *Z. Phys. D*, in print, 1996. <http://xxx.lanl.gov/cond-mat/9610118>
- [17] O. Schapiro, P.J. Kuntz, K. Möhring, P.A. Hervieux, M.E. Madjet, and D.H.E. Gross. Fragmentation phase transition in atomic clusters III — coulomb explosion of cold clusters. *HMI-preprint*, in preparation, 1996.
- [18] D.H.E. Gross and M.E. Madjet. Fragmentation phase transition in atomic clusters IV — the relation of the fragmentation phase transition to the bulk liquid-gas transition. *HMI-preprint*, in preparation, 1996.
- [19] P.A. Hervieux and D.H.E. Gross. Evaporation of hot mesoscopic metal cluster. *Z. Phys.D*, 33:295–299, 1995.
- [20] C.B. Alcock, M.W. Chase, and V.P. Itkin. *J. Phys. Chem. Ref. Data*, 23:385, 1994.
- [21] O. Knacke, O. Kubaschewski, and K. Hesselmann (Eds). *Thermodynamical Properties of Inorganic Substances I, Second Edition*. Springer, Berlin u. Heidelberg, 1991.
- [22] N. Ju and A. Bulgac. *Phys. Rev. B*, 48:2721, 1993.
- [23] S. Frauendorf. Evaporation rates for liquid clusters. *Z.Phys.D*, 35:191, 1995.
- [24] D.H.E. Gross and H. Kalinowski. On the mechanism of heavy ion collisions leading to a compound system and to deep inelastic reactions. *Phys. Lett*, 48 B:302, 1974.

- [25] S.L. Lai, J.Y. Guo, V. Petrova, G. Ramanath, and L.H. Allen. Size-dependent melting properties of small tin particles: Nanocalorimetric measurements. *Phys. Rev. Lett.*, 77:99, 1996.
- [26] M. Seidel and J.P. Perdew. *Phys. Rev. B*, 50:5744, 1994.
- [27] Ph. Dugourd, D. Rayane, P. Labastie, B. Vezin, J. Chevaleyere, and M. Broyer. *Chem. Phys. Lett.*, 197:433, 1992.
- [28] M.M. Kappes, M. Schär, U. Röthlisberger, G. Yeretzian, and E. Schumacher. Sodium cluster ionisation potentials revisited: Higher-resolution measurements for na_n ($n < 23$) and their relation to bonding models. *Chem. Phys. Lett.*, 143:251, 1988.
- [29] M.M. Kappes, M. Schär, P. Radi, and E. Schumacher. *J. Chem. Phys.*, 84:1863, 1986.
- [30] W.A. de Heer, W.D. Knight, M.Y. Chou, and M.L. Cohen. *Solid State Phys.*, 40:93, 1987.
- [31] C. Bréchignac, Ph. Cahuzac, F. Carlier, and M. de Frutos. Shell effects in fission of small doubly charged lithium clusters. *Phys. Rev. B*, 49:2825, 1994.
- [32] B. Cabaud, A. Hoareau, P. Nounou, and R. Uzan. *Int. J. Mass. Spectrom. Ion. Phys.*, 11:157, 1973.
- [33] W. Sundararajan and V. Kumar. *J. Chem. Phys.*, 102:9631, 1995.
- [34] R.C. Weast. *CRC Handbook of Chemistry and Physics, 58th edn.* The Chemical Rubber Company, Cleveland, 1977.
- [35] H.B. Michaelson. *J. Appl. Phys.*, 48:4729, 1977.
- [36] L.S. Wang, Y.T. Lee, D.A. Shirley, K. Balasubramanian, and P. Feng. *J. Chem. Phys.*, 93:6310, 1990.
- [37] K.P. Huber and G. Herzberg. *Molecular spectra and molecular structure, Vol.4.* Van Norstand, Princeton, 1979.

- [38] I. Boustani, W. Pewestorf, P. Fantucci, V. Bonacic-Koutecky, and J. Koutecky. *Phys. Rev. B*, 35:9437, 1987.
- [39] R. Poteau and F. Spiegelmann. *J. Chem. Phys.*, 98:6540, 1993.
- [40] J. Flad, G. Igel, M. Dolg, H. Stoll, and H. Preuss. *Chem. Phys.*, 75:331, 1983.
- [41] G. Burns. *Solid State Physics*. Academic Press, Oxford.
- [42] F. Carlier. *Ph.D.-thesis, university of Orsay*, 1991.

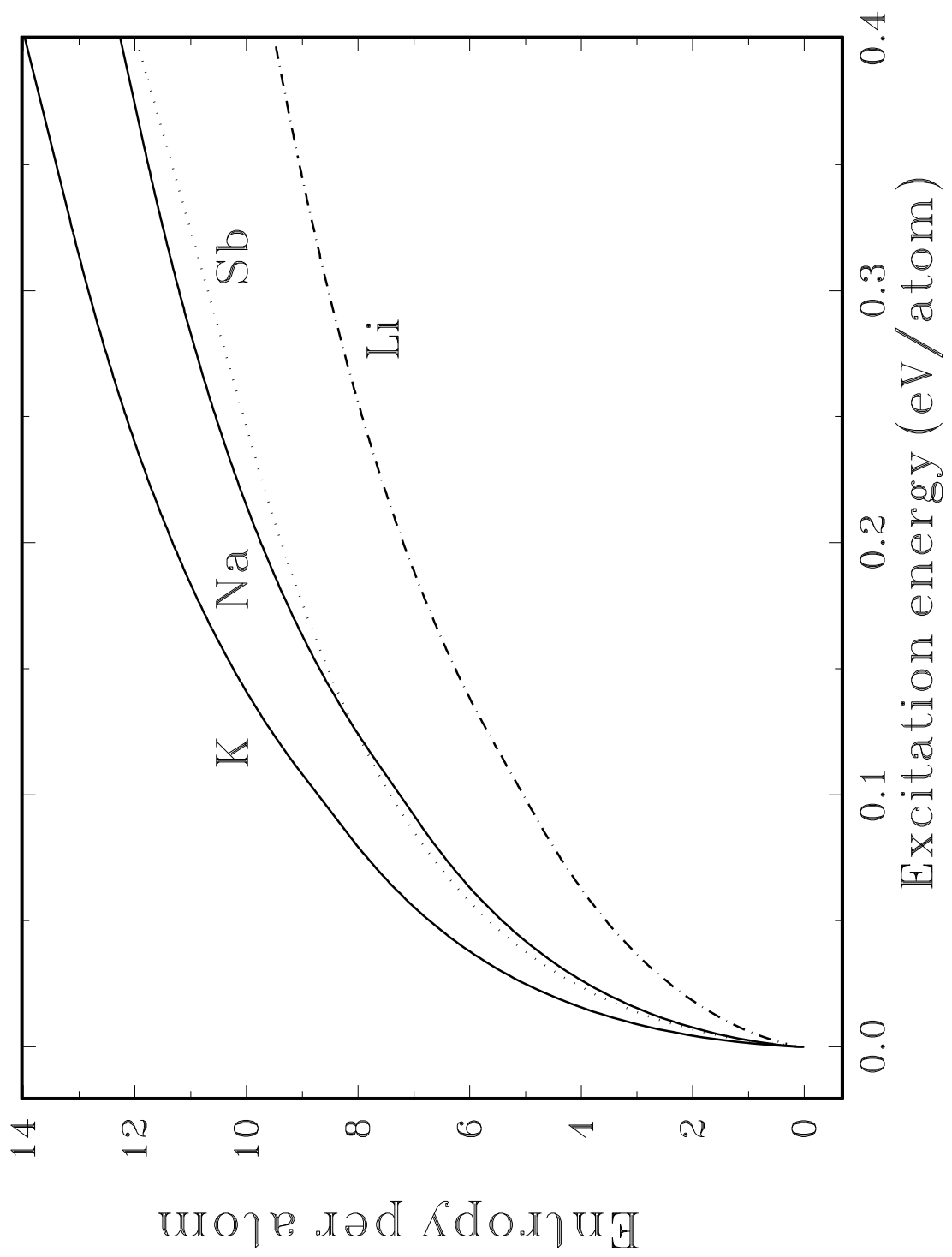


fig. 1

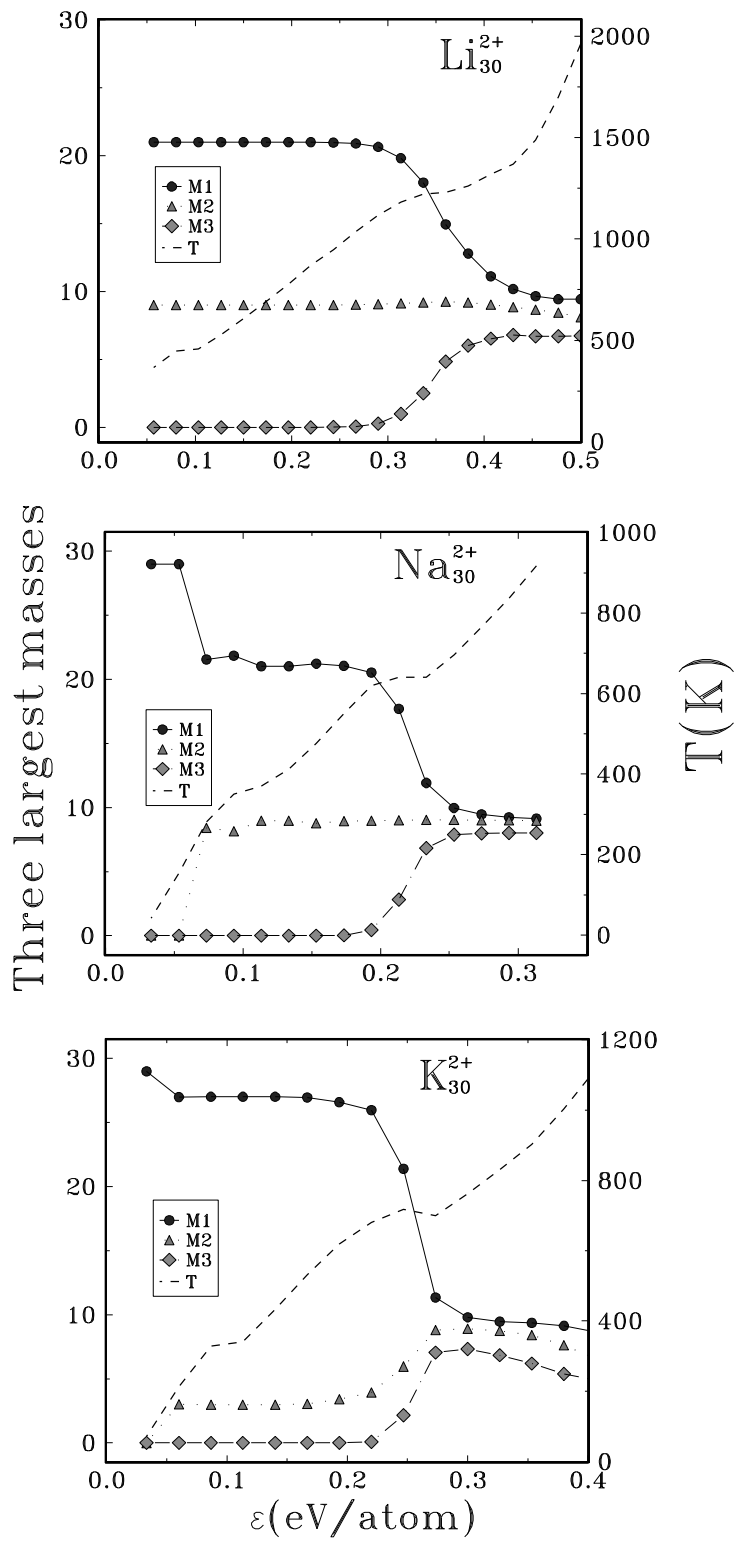


fig.2

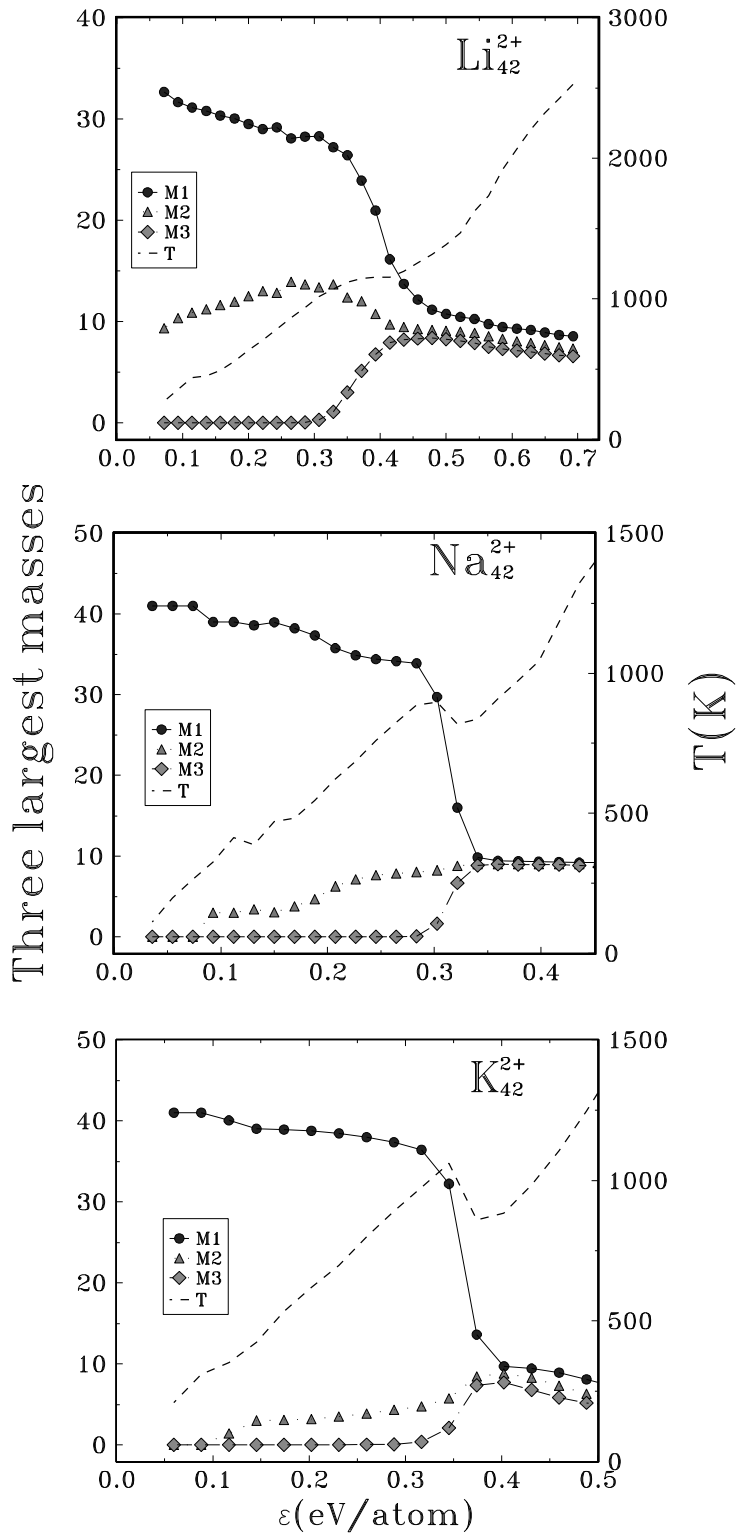
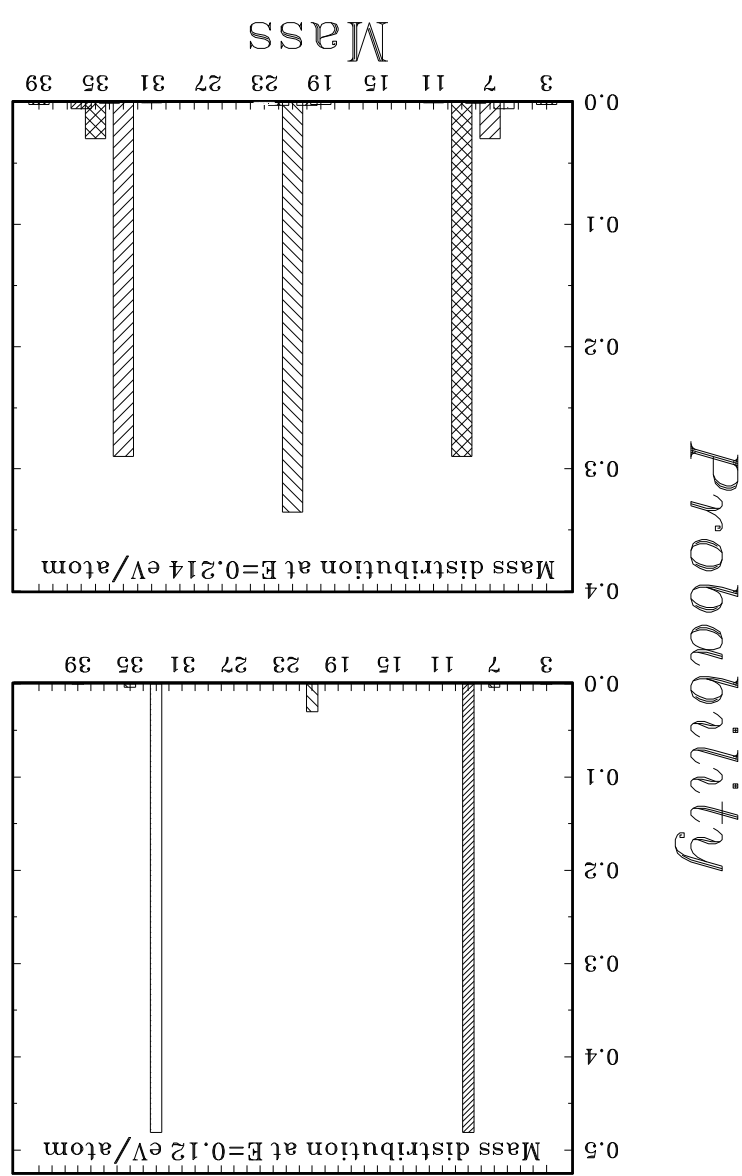


fig.3

Fig. 4



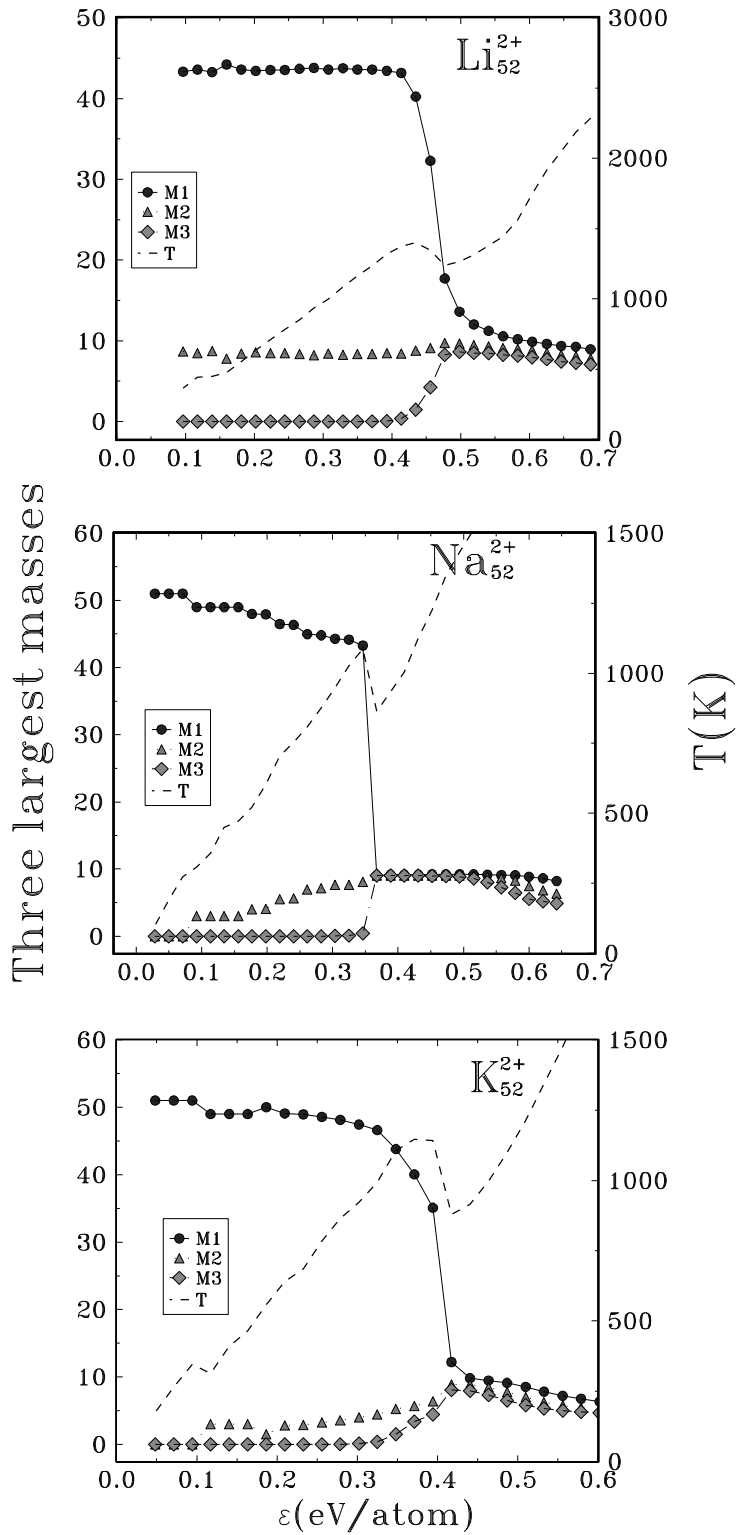


fig. 5

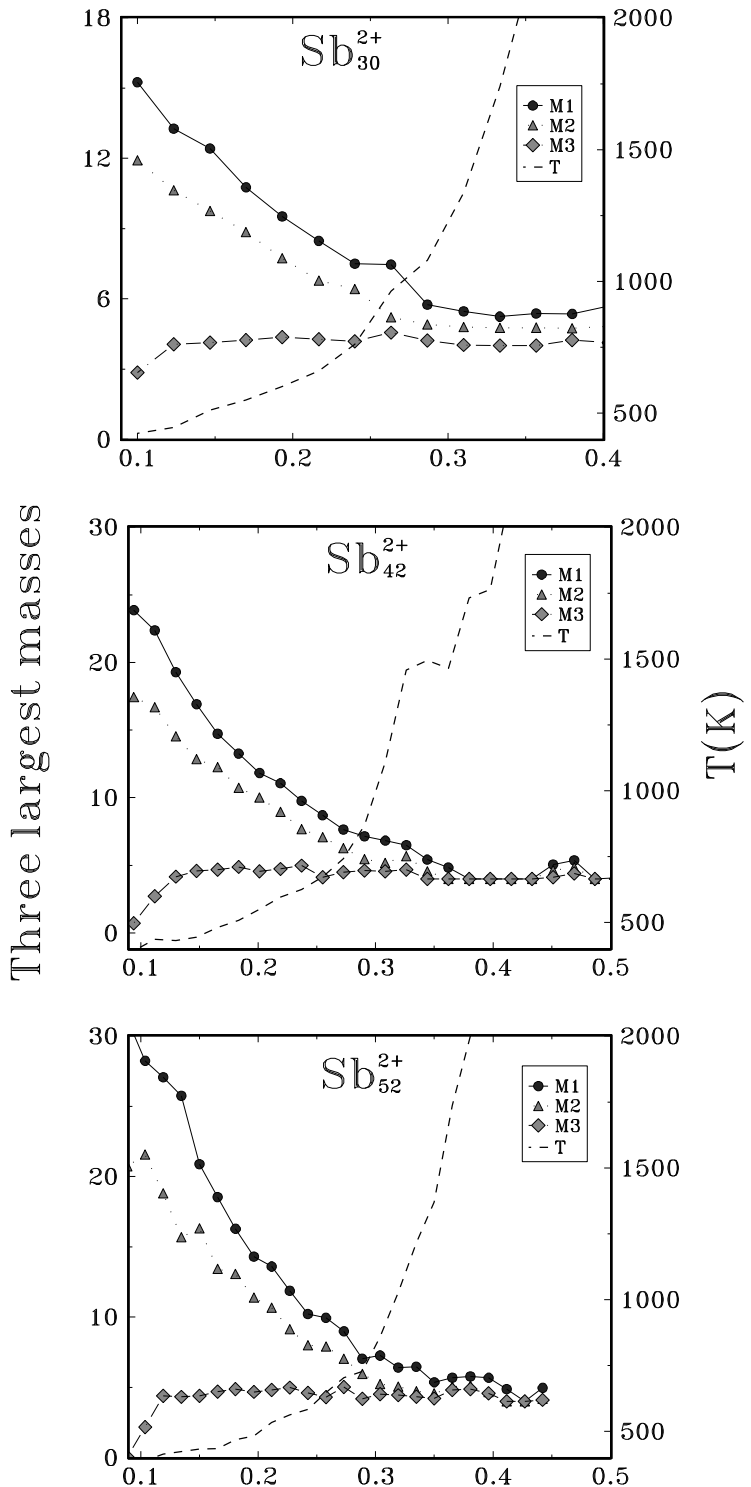


fig. 6

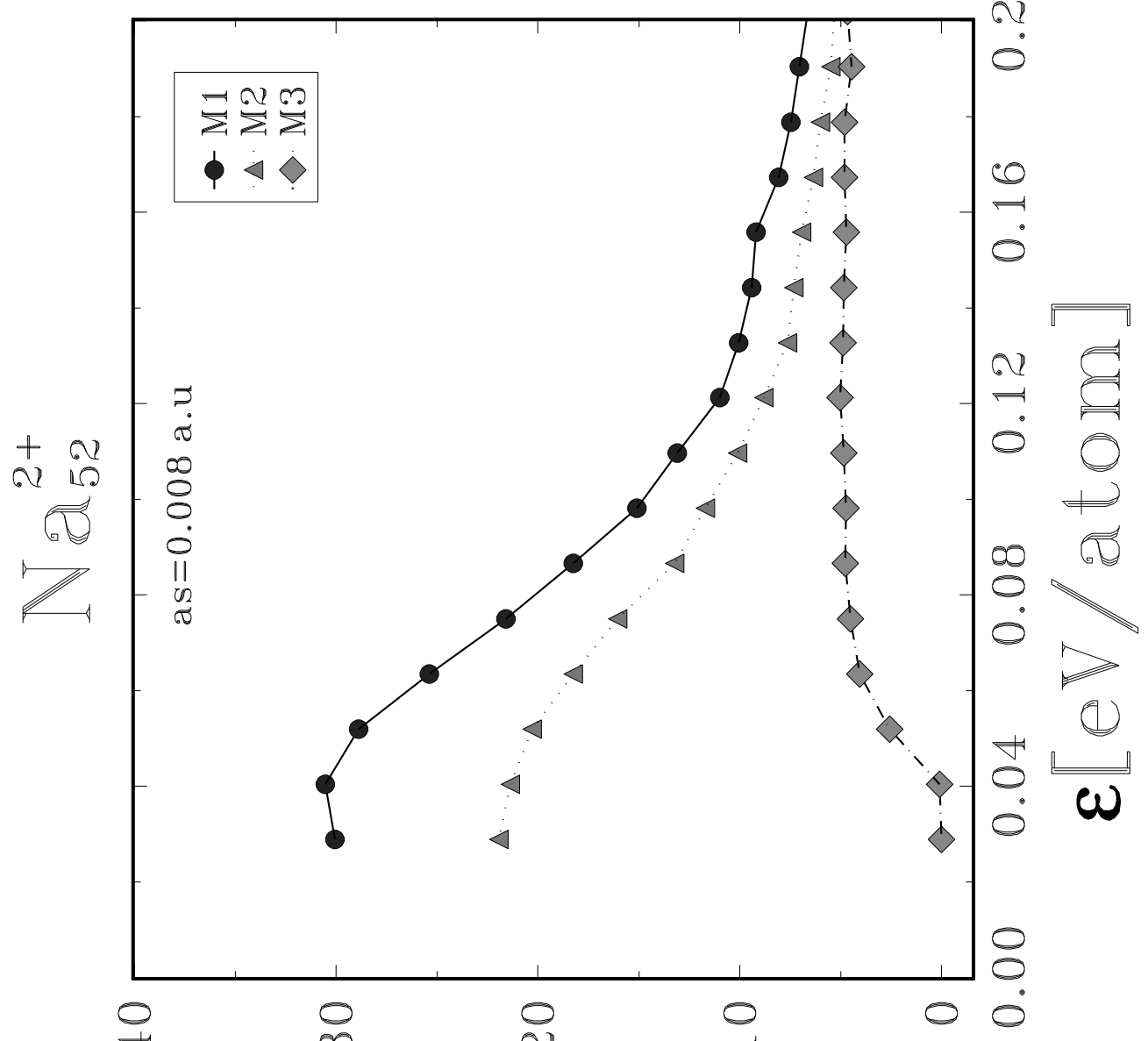


fig. 7